Synthesis and optimization of energy integrated advanced distillation sequences

Li, Qing; Finn, Adrian J.; Doyle, Stephen J.; Smith, Robin; Kiss, Anton A.

DOI
10.1016/j.seppur.2023.123717

Publication date
2023

Document Version
Final published version

Published in
Separation and Purification Technology

Separation and Purification Technology 315 (2023) 123717

Contents lists available at ScienceDirect

Separation and Purification Technology

journal homepage: www.elsevier.com/locate/seppur

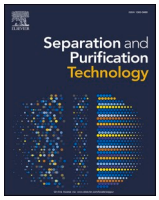

Synthesis and optimization of energy integrated advanced distillation sequences

Qing Li [a,b], Adrian J. Finn [c], Stephen J. Doyle [b], Robin Smith [b], Anton A. Kiss [a,*]

[a] Department of Chemical Engineering, Delft University of Technology, Van der Maasweg 9, 2629 HZ Delft, the Netherlands
[b] Centre for Process Integration, Department of Chemical Engineering, The University of Manchester, Sackville Street, Manchester M13 9PL, United Kingdom
[c] Costain, Costain House, 1500, Aviator Way, Manchester Business Park, Manchester M22 5TG, United Kingdom

ARTICLE INFO

Keywords:
Distillation sequencing
Process synthesis
Process design
Energy integration
Process optimization

ABSTRACT

This paper explores the basis on which reliable screening of distillation sequences for energy-efficient separation of zeotropic multicomponent mixtures can be carried out. A case study for the separation of natural gas liquids is used to demonstrate the approach. To solve this generic problem, a screening algorithm has been developed using optimization of a superstructure for sequence synthesis using shortcut models, in conjunction with a transportation algorithm for the synthesis of the heat integration arrangement. Different approaches for the inclusion of heat integration are explored and compared. The best few designs from this screening are then evaluated using rigorous simulation. It has been found that separation problems of the type explored can be screened reliably using shortcut distillation models in conjunction with the synthesis of heat exchanger network designs. Non-integrated designs using thermally coupled complex columns show much better performance than the corresponding designs using simple columns. However, once heat integration is included the difference between designs using complex columns and simple columns narrows significantly.

1. Introduction

The rise in worldwide energy usage has increased interest in cost-effective ways of reducing energy use. Distillation is by far the most widely applied separation technology, but it is recognized as the most energy-intensive operation in the chemical industries due to its inevitable energy degradation. Distillation processes can use one or more distillation columns. For instance, to efficiently separate multicomponent mixtures into more than two product streams using distillation, a sequence of distillation columns is required, which results in significant energy demand and associated CO_2 emissions. Because of its configuration complexities related to process energy efficiency, studies of distillation synthesis have been developed over the past decades to bring cost-efficient solutions. Early work was carried out by Seader and Westerberg [1] and Andrecovich and Westerberg [2].

1.1. Distillation sequence synthesis

The number of possible sequences is large. For example, for a five-product mixture separation using simple columns only, there are 14 possible sequences, but this number rises to 4862 when the number of products is 10. The number of possible sequences is greatly increased with the number of products from fractionation units. The increase in the number of fractionation products leads to extensive sequence options when only simple columns are used, but this number grows exponentially if thermally coupled complex column options are further considered.

Mathematical programming has been developed to achieve automated distillation sequence synthesis. It commonly formulates the design problem through representing the number of possible sequences to separate multicomponent mixtures, and obtaining the optimal sequence with detailed process design. Due to the non-linearity, non-convexity and increased problem sizes for large-scale distillation sequence synthesis problems, it is challenging to find an optimal sequence configuration solution with an acceptable computational time. Different studies focus only on attempting to synthesize all possible distillation configurations for a multicomponent separation problem using superstructure optimization, separation matrix methods, or simultaneous heat and mass integration methods [3–5].

Applying distillation sequencing heuristic rules to reduce the search space would be one way of solving the issue. For example, Lee et al. [6] removed plentiful components at the end of the sequence to narrow the

* Corresponding author.
E-mail address: a.a.kiss@tudelft.nl (A.A. Kiss).

https://doi.org/10.1016/j.seppur.2023.123717
Received 1 February 2023; Received in revised form 24 March 2023; Accepted 27 March 2023
Available online 31 March 2023

sequence possibilities. But promising solutions could be missed because simultaneous optimization cannot be achieved based on all possibilities. Other work handled this large problem by retrofitting of an existing distillation system [7,8] or by sensitivity analysis in which one variable is changed parametrically while other variables are fixed [9]. But these methods are based on fixed operating conditions, and thus cannot obtain the optimal operational solutions and may miss optimal operating parameters. Zhang et al. [10] proposed a task-based program method followed by a simulation–optimization model to carry out optimal design for distillation sequences. However, the task-based method does not allow operating conditions to be changed in different sequences and thus loses design degrees of freedom. Leeson et al. [11] presented an MILP optimization to determine the optimum separation sequence within a reduced process superstructure at a conceptual design stage, but only simple columns are considered in their work.

The method most often used to address larger problems is to use shortcut distillation models to screen the large number of structural options and determine the best few potential designs to reduce the search space, followed by more detailed examinations of the best few designs using rigorous simulation [12,13]. Convergence guaranteed shortcut methods are developed to fast screen the search space of non-heat integrated distillation sequences and their efficacy is further rigorously evaluated. However, excess stages were introduced to the Aspen Plus rigorous model when it was used to evaluate their shortcut method by comparing the heat duty requirements of the two methods [12]. To simplify the models, there are also some assumptions made on key operating variables. For example, all column pressures are assumed to be the same throughout the sequence, using relative volatilities of the initial feed for all columns. It is therefore unclear whether shortcut distillation models have the necessary accuracy for reliable screening.

The thermally coupled complex columns based on the principle of process intensifications are then applied to distillation sequences to reduce the remixing of non-key components, and thus lead to a more energy efficient separation sequence and are potentially able to reduce both operating and capital costs [14,15]. Among the complex columns, dividing-wall columns (DWC) are the most common options studied as a complex column application in distillation sequence synthesis cases [6,16–18]. Their results show the use of DWC can bring energy savings and capital cost savings (up to 50%) compared with simple columns. Nevertheless, the use of DWCs may also require distillation at non-optimal column pressures, and thus may cause more expensive cooling media costs if for example refrigerant is required. Halvorsen et al. [16] reported that using a DWC to substitute the original two simple columns for a natural gas liquid process might reduce the size of the columns as well as the carbon footprint, but it will increase the refrigerant requirement at an even lower temperature than in simple columns. Therefore, whether or not to apply DWC to replace simple columns should be decided based on an optimisation. There are also other complex column options which may benefit the distillation sequences in terms of energy savings. For example, Agrawal and Fidkowski [19] reported that the side columns may provide efficient configuration more often when compared with the fully coupled column configuration. Thus, the use of all complex column options should be determined within the sequence synthesis, but few have been studied in a distillation sequence systematically. Waltermann and Skiborowski [20] and Skiborowski [21] proposed optimization approaches for the synthesis of energy integrated distillation processes including various simple and complex column options. But in their work, the processes include only three products, meaning that either two simple columns or one complex column is needed without demanding a distillation sequence, thus the problem size is reduced.

1.2. Integration of sequence synthesis with complex options

Heat integration and column operating conditions generate design degrees of freedom and they interact with each other. In distillation sequences, the large amount of energy required by the system creates a wide temperature range and significant quality of heat sources in the columns, which can provide potential heat integration opportunities. The energy requirements and heat sources in the sequence affects column operating conditions and column geometries and the choice of operating conditions for the columns affects not only the design of a column but also influences columns thermodynamic characteristics (i.e. operating temperature and heat flow rates) and thus influences heat integration opportunities. For instance, the column operating pressures might be increased to create heat integration opportunities (e.g. to increase the condenser temperature). In turn, the heat integration also affects the column operating conditions (e.g. feed conditions and reflux ratio). Therefore, the operating conditions and heat integration opportunities should be optimized simultaneously together with the distillation sequence synthesis.

The other reason for the simultaneous heat integration is that if heat integration is introduced based on a previously fully designed process, which may result in the omission of competitive solutions and unfair process comparisons [22]. Potential heat integrated structures prior to parameter optimization require an exhaustive enumeration which is time-consuming. Therefore, to enhance the energy efficiency of the distillation systems, it is required to manipulate not only the arrangements of sequences, but also the heat integration with operating conditions and column configurations simultaneously. An et al. [23] generated a method to search heat-integrated distillation sequences, but only simple columns are considered. Zhang et al. [24,25] enhanced this method to synthesize more complex processes considering heat-integrated and thermally coupled distillation sequences. However, some key operating conditions, e.g. feed conditions and column pressures, are not included. Zhang et al. [10] proposed a sequence optimization without heat integration considering the number of stages, feed stage locations, and operating conditions. So far, the previous approaches still cannot provide a solution that considers these complex options concurrently.

Overall, the greater number of interconnected design variables in distillation columns increases the design complexities significantly in terms of structural representation and the more complex combinatorial problem when sequence synthesis, column operating conditions and heat integration are all considered, and produce a more challenging non-linear optimization problem [26]. To find a solution for any process design problem, many sequences with different operating conditions must be examined from a process integration perspective, and therefore an integrated systematic approach is required to provide reliable distillation sequence synthesis and design optimization. A recent paper [27] developed mathematical programming based approaches to identify the most energy-efficient distillation configuration sequence for a given separation, and a more detailed review on introducing thermally coupled columns into distillation sequences can be found [28]. However, these studies focus on the perspective of generating more efficient thermally coupled column possibilities, rather than optimizing the whole distillation sequence together with allowing changes of condenser types, feed qualities, heat pumping (refrigeration), etc. at a flowsheet level. It is so far not clear whether shortcut models have the required accuracy for reliable screening of sequences. Furthermore, it is also unclear whether the heat integration can be represented by the energy targets of pinch analysis with maximum heat recovery, or whether it is necessary to produce detailed heat exchanger network designs for screening. Additionally, although the thermally coupled complex columns have the possibility to bring energy savings, the combination of the two simple columns also loses degrees of freedom by heat integration between different columns. When heat integration is taken into account, the potential heat integration possibilities for complex columns decrease as the combination of heat sinks and sources are constrained. It is not clear how much difference the benefit of heat integration makes to complex columns and simple columns, and thus it is difficult to make an optimal selection for using complex columns if heat integration is

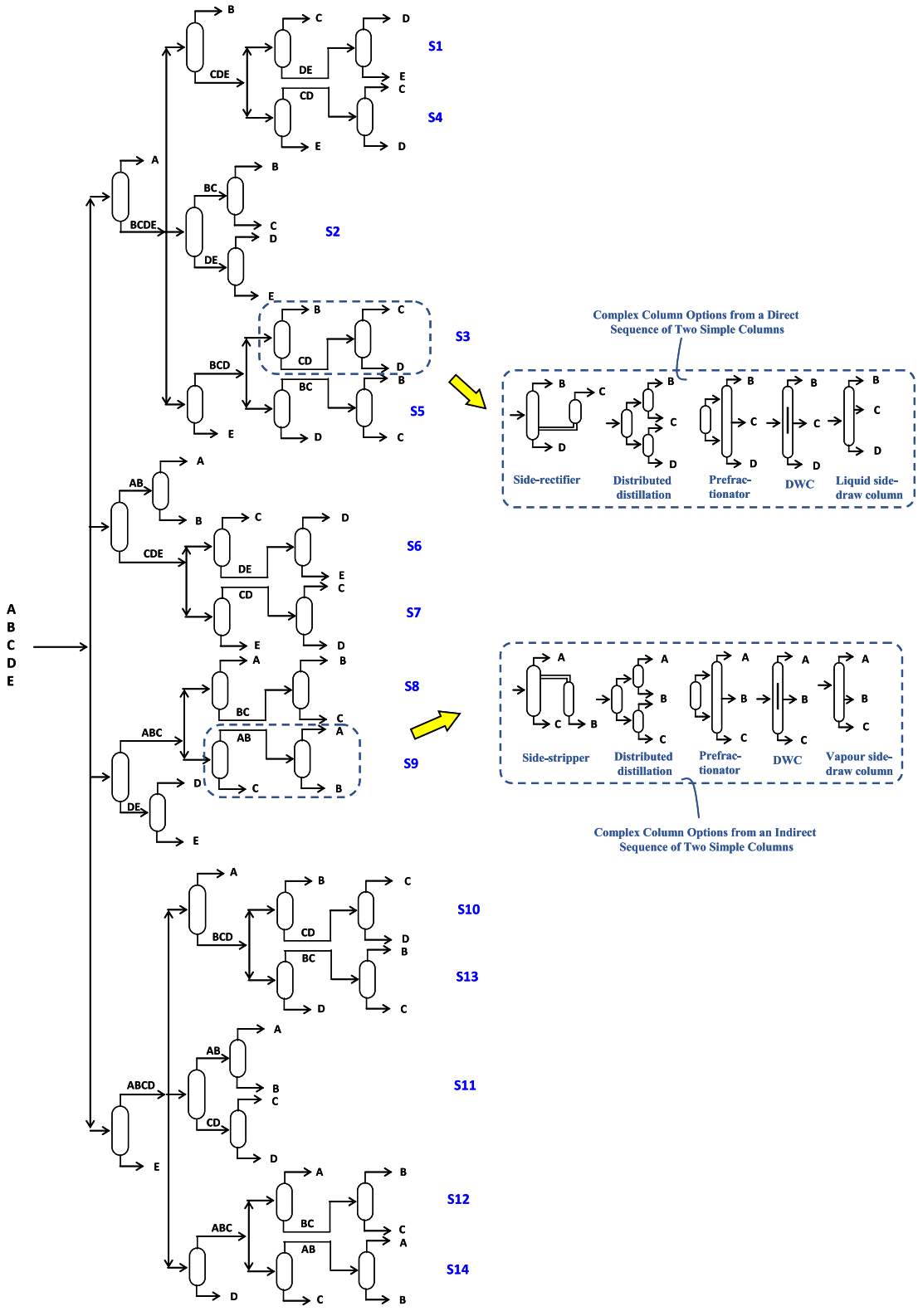

Fig. 1. Superstructure for the optimisation of distillation sequences [30].

considered.

The novel contribution of the present research is to develop a systematic approach (using a quick screening method combined with optimization) for the advanced distillation sequences used on combinations of energy-efficient complex columns (side-strippers, side-rectifiers, side-stream columns; and prefractionation arrangements, including Petlyuk columns and dividing wall columns) by eliminating simplifying assumptions and simultaneously including all degrees of freedom, such as column design parameters and operating conditions (feed condition; pressure; condenser type). Furthermore, for the first time this work addresses heat integration explicitly for a complex sequence optimization by generating a heat exchanger network (HEN)

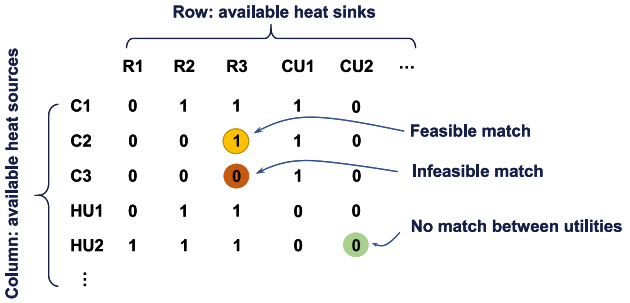

Fig. 2. Heat integration model embedded into superstructure.

Table 1
Decision variables (degrees of freedom) in the distillation sequence optimization.

Type	Variables	Constraints / Bounds
Integer variables	Sequence number	n/a
	Column merge (to form complex columns)	n/a
	Column merge type	n/a
	Condenser type	Total or Partial
	Side stream quality	Liquid or Vapour
Continuous variables	Column feed pressure	1 bar–0.95 × feed critical pressure
	Column feed quality	0–1
	Reflux scale up (R/R_{min})	1.1–5

configuration that accounts for practical constraints, via a matrix representation (rather than using Pinch Analysis). An industrial case study, NGL fractionation system optimization, is used to demonstrate the methodology proposed in this work.

2. Problem statement and motivation

The optimization of the distillation sequence systems is motivated by the benefits of energy savings in reducing costs and CO_2 emissions. Its design requires many interconnected design degrees of freedom, which lead to a challenging optimization problem. Reaching high quality distillation sequences from mathematical optimization, including integration with complex options, simple columns, complex columns, heat integration with heat exchanger network design, adjustment of operating conditions, has been shown to be complicated and time-consuming for large-scale problems. Using heuristics in the past often led to an economically viable solution, but may miss promising sequences, particularly for updating new and complex options. Complex column options that overcome remixing effects, do have value but have not been studied in detail. Thermal integration has been studied, but not with so many column options nor with a methodical and robust optimization approach.

This study addresses this problem by combining process synthesis and optimization to evaluate all the fractionation process alternatives, as illustrated by a natural gas liquids (NGL) separation case study. Shortcut distillation models are used for fast screening, which determines which possible sequences are likely to achieve the desired separation, eliminating simplifications on key design variables. A process optimization procedure is then used (based on simulated annealing) to find and rank the best configurations in terms of total operating cost.

3. Methodology and optimization approach

3.1. Superstructure sequences synthesis approach

Taking advantages of a superstructure, all possible separation sequences for a given multi-component mixture can be derived, and the basic superstructure can also be extended with advanced options in mathematical ways. For a given mixture of (P) products, the number of simple column sequences (S) is given by the formula: S = [2(P-1)]! / P! (P-1)! [29]. This basic superstructure is then extended to handle complex column options. In principle, any two column tasks in the superstructure can be merged to give different complex column arrangements. As shown in Fig. 1, a three components mixture separation task represented by the circled two simple columns has the potential be achieved by alternative thermally coupled composite columns with a single feed and three product streams (side-stripper, side-rectifier, pre-fractionators, and thermally coupled pre-fractionators, liquid side draw, vapor side draw) [30].

The appropriate complex column arrangement options depend on whether the two simple columns in the series are in the direct or indirect sequence. For a 5 component mixture, there are S = 14 simple column sequence possibilities. Taking simple column sequence 1 (S1) as an example. The separation task order is: A/BCDE, B/CDE, C/DE, D/E. Based on this separation task, the optimizer tries several paths to select various complex columns, and finally when the optimization converges, the optimal complex column sequence is produced based on the sequence 1 separation task. The simple column sequences and the corresponding complex column sequences are optimized based on the same starting defaults. Therefore, this generated optimal complex sequence is actually not the only configuration possible or evaluated, but rather it is the optimal solutions found by the optimiser after optimising all the possible combinations of complex columns, based on the simple column sequence 1 structure (i.e. performing the same separation tasks). Other optimal complex column sequences are also determined in the same way. Each simple sequence has 4 simple columns, and each complex column could contain 2 complex columns or 1 complex column and 2 simple columns. The shortcut Fenske-Underwood-Gilliland (FUG) models are used to design the columns and can screen very many options. These models can avoid dramatic computational difficulties created by nonlinear, large tray-based combinations of rigorous design formulation and provide an efficient screening for a large number of separation sequences [31–33]. Rigorous simulation can then be carried out based on the attractive sequences, as screened and selected by shortcut models.

3.2. Process heat integration

During operations in the chemical process sector, a large amount of heat is consumed in separation systems, which brings considerable heat across the processes with a wide range of temperatures under different operating pressures, and thus creates potential opportunities for heat recovery. Before optimisation can be applied to the superstructure, the energy cost is evaluated for each structure and set of conditions. Energy integration options are thus applied to each sequence during the optimisation process to enhance process energy efficiency. This requires optimisation of the matches between heat sources (defined as hot streams discharging energy) and heat sinks (defined as cold streams absorbing energy) throughout the process to be determined. The match between a heat source and a heat sink can be considered through a heat exchanger with a feasible temperature difference. Heat integration opportunities including feed preheating or precooling and column to column heat recovery (between column condensers and reboilers) are optimized with sequence synthesis simultaneously. As shown in Fig. 2, all heat sinks and heat sources are compiled into an incidence matrix, and are solved by using an MILP transportation model [34,35]. A heat exchanger network can be synthesized for each separation sequence. Binary variables are introduced to make discrete decisions for each match between rows and columns of the matrix. Closed cycle heat pumping is also taken into account in this optimisation to divert heat to above ambient cooling water to further achieve energy savings when a sub-ambient utility media is required [36,37].

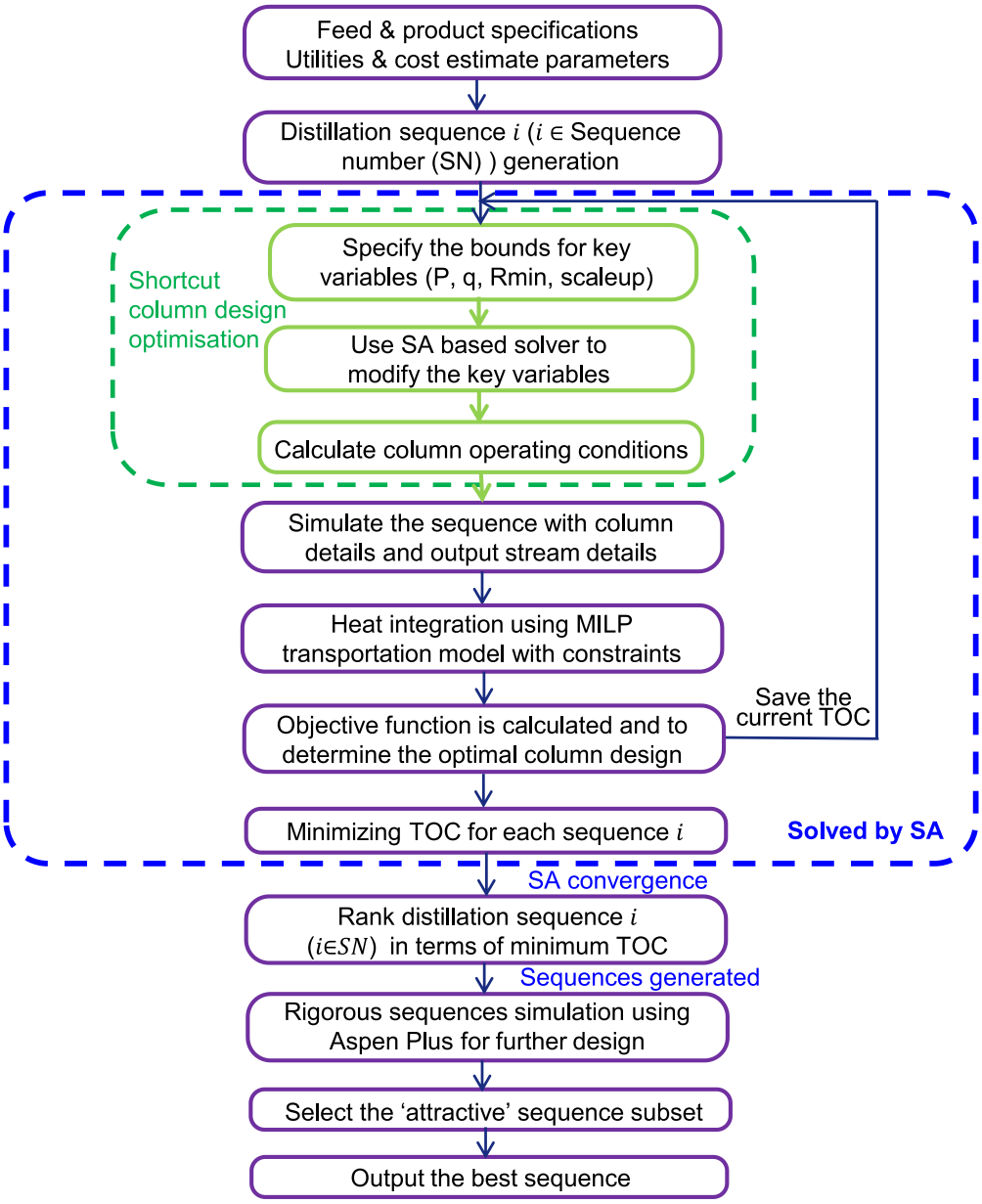

Fig. 3. Framework of the optimization method for distillation sequences design.

3.3. Design variables and interactions

To eliminate the assumptions on key design decision variables in the previous literature, the proposed approach allows adjustment of the column pressure, condenser type, reflux scale-up, reflux ratios, feed conditions, and complex column options, together with heat integration opportunities to achieve an integral optimization and find the optimum operating conditions, as listed in Table 1.

- Sequence number. Each sequence number represents a different order of separation tasks, the optimization of which can lead to different outcomes. For example, heuristic rules suggest doing the most difficult separation last, because a difficult separation requires a high reflux ratio. However, the most difficult separation can also be carried out earlier. This is because separating the most difficult binary pair in the presence of non-critical components greatly increases the vapor and liquid flow rates in the column and correspondingly increases the energy required for separation. However, when the relative volatility is small between a binary pair, the relative volatility between the components can be enhanced by the addition of a third component to increase the relative volatility between the close boiling binary pair through differential molecular interactions. The relative volatility between the components is not constant throughout the separation, and is influenced by the change of mixtures to separate and by the change of conditions. Of these opposing effects, whichever is dominant depends on the details of the individual separation, and thus an optimization is needed to find the best conditions.
- For column pressure, an increase in the column pressure increases the stream (column distillate or bottom product) temperatures. If a stream that needs to be condensed is only matched by a low-temperature refrigerant, increasing the column operating pressure may be optimized to increase the temperature so that cooling water can be used instead. Thus, the operating pressure can be determined to match the available utilities or the hot and cold utilities for the condenser and reboiler can be assigned for fixed pressure. In addition, the change of operating pressure should be optimized together with heat integration. Heat integration by closed-loop heat pumps is

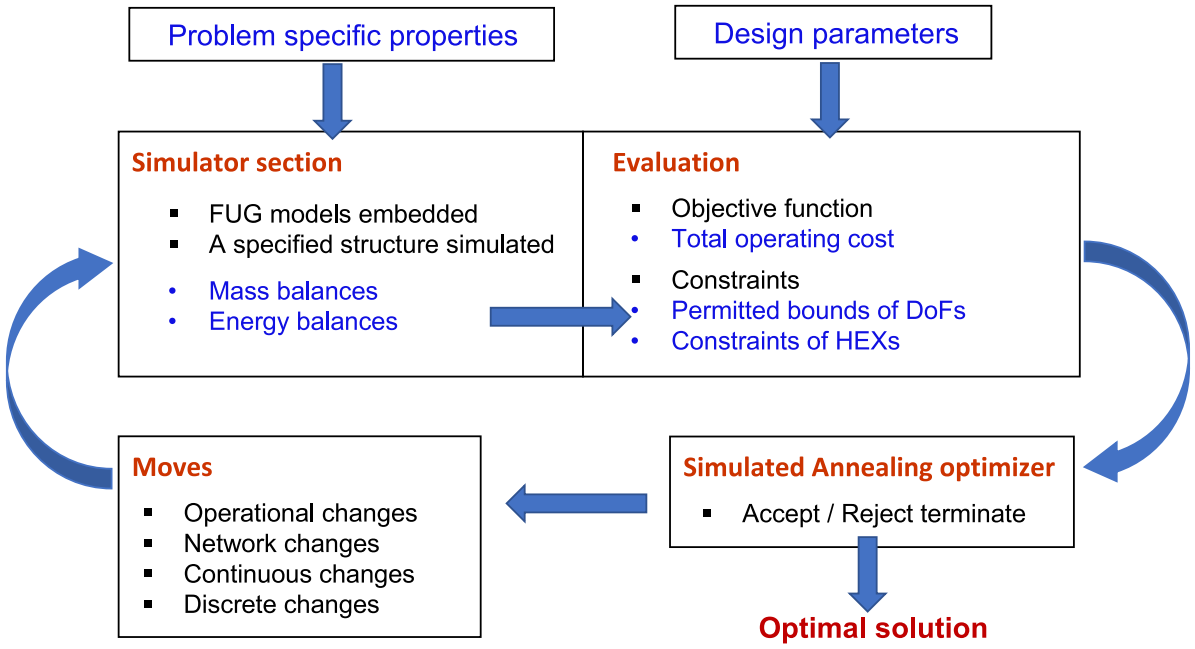

Fig. 4. Framework for Simulated Annealing optimization procedure.

used simultaneously to investigate its association with the sequence energy efficiency.

- For reflux ratio and reflux scale up (the ratio between the actual reflux ratio and the minimum reflux ratio): reflux ratio not only affects the individual column, but also impacts heat integration by affecting condenser and reboiler duties. The relative volatility varies accordingly with the column pressure.
- For condenser type and feed conditions: either partial or total condensers are selected. The feed conditions (including pressures, temperatures and feed quality) for each column are optimized, and are considered independently of the column pressures, depending upon the permitted feed quality, which could be sub-cooled, two phase or super-heated. No additional pressure drop is considered for any feed stream heat exchangers.

3.4. Process optimization

3.4.1. Optimization approach

In this work, a decomposition method is proposed to solve this complex optimization problem, as shown in Fig. 3. For the given feed mixtures, distillation sequences are first generated by the proposed superstructure with defined operating conditions. The key decision variables are specified within their bounds and are then optimized by the optimizer to design the distillation columns in sequences using the shortcut models. The sequences with specific design operating conditions are then generated with column details and the stream details are then outputted for heat exchanger network synthesis. The outputs of stream temperatures, heat capacities, heat integration opportunities are explored, and the optimal heat exchanger network structure is conducted in terms of the energy target. Heat exchangers are assumed to connect in parallel without a series of exchangers in an individual stream, which means that multiple exchangers acting as a condenser or reboiler have the same inlet and outlet temperatures, i.e. for a total condenser, $T_{in} = T._{dew}$, $T_{out} = T._{bub}$. Heat exchangers connecting in parrel also avoids the high non-linearity introduced by the intermediate temperature because of the log mean temperature difference (LMTD) calculation for each HEX in the series. The shortcut distillation model equations are embedded in a column sequence simulator, rather than the optimizer, with operating conditions adjusted by the optimizer. The overall decomposed simulation-based optimization is achieved using a mixed-integer linear programming (MILP) formulation inside the Simulated Annealing (SA) algorithm.

The optimization framework is given in Fig. 4. The SA optimizer creates 'moves' in the optimization that allow for changes in the distillation structure (e.g. changing two adjacent column tasks to be a complex column task) and the decision variables (e.g., P, q, Rmin, reflux scale-up) within their permitted bounds. They are taken as inputs for the shortcut distillation models. After each move, the sequence is then simulated, the objective function is evaluated, constraints violation checked, HEN designed, and the corresponding total operating cost is estimated. The objective function value is then sent back to the optimizer. The optimization method then changes the decision variables and repeats the process until convergence is obtained, based on annealing parameters. A hierarchy of sequences can be determined by repeating the optimization using additional constraints to reject any previous solutions. This hierarchy can be used to identify promising sequences that can be further evaluated. The annealing parameters used are: random number generator seed (2); initial and final annealing temperatures (10^{9} and 10^{-8}); Markov chain length (70); maximum iterations (25,000); maximum consecutive failed chains (10); maximum unsuccessful moves (300); cooling parameter (5×10^{-3}) and move acceptance criterion (Metropolis).

The objective function of the optimization in this work is the minimum operating cost, which is directly proportional to the energy used in the process. A fair question at this point is: why not the total annual cost? This is because taking into account the capital cost requires using the same correlations for both simple and complex columns, without any inconsistencies. There are no generally accepted simple capital cost correlations available for different complex column arrangements to allow a consistent comparison. Another problem is that of using the annualized capital cost to obtain a total annual cost. For example, assuming an annualization of 5 years versus 10 years will give a completely different balance between capital and operating costs. Thus, simply adjusting the annualization factor can lead to different results in the optimization. Whilst we can be reasonably scientific about utility costs, which are directly proportional to the energy used in the process, capital cost cannot be dealt with in the same rational way. When the capital costs need to be taken into account, the top results of the optimal

Table 2
Design specifications in the optimization calculations.

Parameters	Value/unit
Heat transfer coefficient in the reboiler and condenser	600 W/m^{2}K
Minimum temperature difference	10 °C
Ambient temperature	20 °C
Sub-ambient minimum temperature difference	4 °C
Default feed quality	q = 1
Compressor maximum size	20,000 kW
Maximum compression ratio Pout/Pin	5
Isentropic efficiency	87%
Liquid pump efficiency	90%
Refrigeration critical pressure fraction	0.8
Annual operating hours	8400 h
Pressure decreasing in columns	0 bar

designs (minimal TOC) can be considered by adding also the annualized capital costs and then checking the total annualized costs to see if the ranking changes. For the sake of completeness, a rough indication of the total investment cost - estimated using the IChemE method [38] - is also provided for the optimal distillation sequences.

3.4.2. *Design specifications*

The options used in the optimization calculations are shown in Table 2. The separation is assumed to be sharp split. Liquids and gases are pressurized by pumps and multistage-compressors and depressurized by valves and turbo expanders. The flowchart of the models of multistage-compressors and turbo expanders are given in Appendix A.

3.4.3. *Optimization tool*

This optimization methodology can be carried out within the ColSeq software developed and available at the Centre for Process Integration of The University of Manchester [39]. This stores the "best" N sequences with the ability to ignore similar structures so that a set of promising sequences can be identified for further evaluation, which can reduce the effects of inaccuracy led by shortcut design models. To the best of our knowledge, the ColSeq software is one of the most advanced available for this task. It can be used not only for process optimization but also for the simulation of each distillation column unit, which closes the gap where previous algorithms did not provide unit operations that were accepted by process engineers in the chemical industry [40]. All complexity options have been included in the process synthesis and optimization panel, e.g. total or partial condenser, feed quality optimization, reflux ratio optimization, pre-fractionator recovery optimization, pressure optimization, multi-stage intercooled compressors, closed cycle heat pumping, dephlegmators, side-strippers, side-rectifiers, (thermally coupled) pre-fractionators, sloppy pre-fractionators, and also dividing-wall columns. These are all optimized simultaneously and systematically. It is the only software we are aware of that is capable of achieving this feat.

4. Case study: Natural Gas Liquids separation

As the energy use of industry and society moves to a more sustainable basis, it is projected that there will be a significant reduction in the use of coal and oil, but a significant growth in the use of natural gas. The International Energy Agency projects that between 2017 and 2040 there will be a 44% increase in the use of natural gas [41]. This growth will be realized by a significantly greater proportion of the natural gas being traded as liquefied natural gas. The raw natural gas typically contains a small, but economically very significant, portion of heavier hydrocarbons. The heavier hydrocarbons have a value significantly greater than the methane as chemical plant and refinery feedstock, and as liquid fuels. These heavier components are separated from the predominantly methane fuel gas as Natural Gas Liquids (NGL), as defined in Fig. 5, composed of ethane, propane, i-butane, n-butane, and a gasoline fraction (pentane and other heavier components). The NGL fractionation is one of the most energy-demanding processes in the oil and gas industry. Once the NGL mixture is recovered from the natural gas stream, it must be separated into relatively pure components to be useful.

The NGL fractionation process typically uses a train of four distillation columns that separates in the order of 2.5 million tons per year of NGL feed, requiring approximately 77 GJ per barrel (0.4 MJ/liter) energy, and is equivalent to 4.65 tons of CO_2 emissions per barrel [42]. Considering the massive scale of operations in NGL fractionation (e.g. 100,000 BPD for a single plant), any energy savings are important and would contribute to fewer greenhouse gas (GHG) emissions because of long-term pressure to move energy production to a more sustainable basis.

Although many improved conceptual designs of NGL recovery processes have been introduced to date to enhance the economics and efficiency [43,13], these designs are still much more complex and far from suitable for industrial practice [44]. Qyyum et al. [44] also carried out an assessment of the NGL recovery processes to provide references and help process design engineers choose conceptual design for further

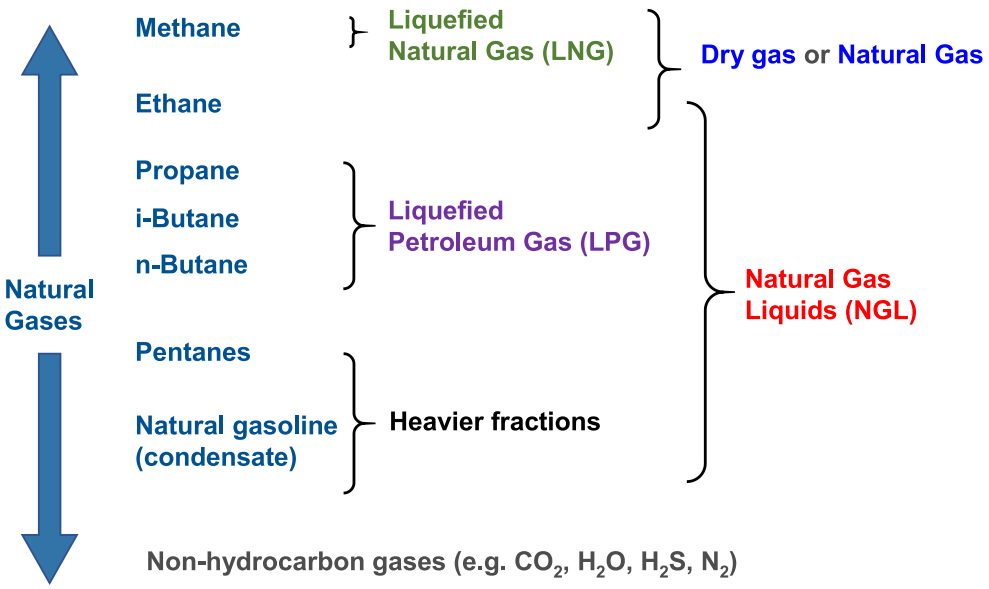

Fig. 5. Difference between NGL, LNG, LPG and NG.

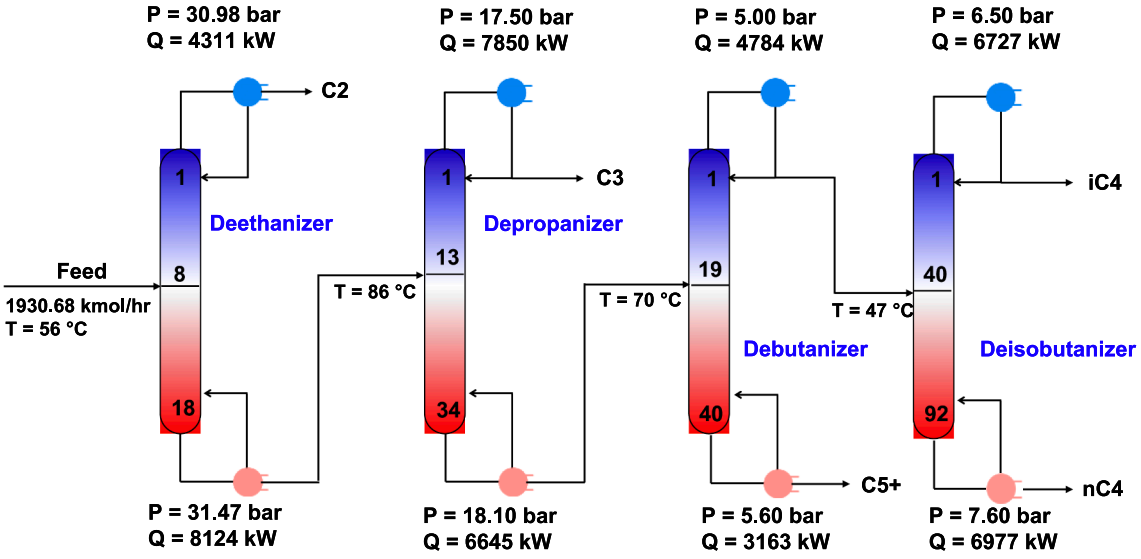

Fig. 6. NGL fractionation in a conventional process [42,8].

Table 3
Feed and product compositions in percentage of liquid volume [8].

Component	n.b.p. (°C)	Feed mol%	Ethane (A)	Propane (B)	I-butane (C)	N-butane (D)	Gasoline (E)
Methane	−161.5	0.5	1.36				
Ethane	−88.5	37.0	95.14	7.32			
Propane	−42.2	26.0	3.50	90.18	2.00		
i-Butane	−11.7	7.2		2.50	96.00	4.50	3.00
n-Butane	−1.0	14.8			2.00	95.00	
i-Pentane	27.8	5.0					33.13
n-Pentane	35.9	3.5				0.50	23.52
n-Hexane	68.5	4.0					26.90
n-Heptane	98.3	2.0					13.45

Table 4
Relative volatilities calculation examples for the NGL feed.

Component		Relative volatilities
C1	Methane	372.98
C2	Ethane	101.55
C3	Propane	38.66
i-C4	i-Butane	19.16
n-C4	n-Butane	14.78
C5+	i-Pentane	7.26
	n-Pentane	5.88
	n-Hexane	2.39
	n-Heptane	1.00

Table 5
Heating and cooling utilities used in the NGL fractionation [45].

Utility	Supply T (°C)	Return T (°C)	Price ($/GJ)
HP steam	255	254	5.66
MP steam	185	184	4.77
LP steam	161	160	4.54
Cold water	20	25	0.378
Chilled water	5	15	4.77
Refrigerant	−21	−20	8.49
Electricity	–	–	18.72

enhancement. Overall, there are still significant improvements that can be made for the synthesis of energy-integrated distillation sequences.

The design details of the conventional NGL fractionation process given in Fig. 6 are the rigorous simulation results obtained from Aspen Plus, based on the reported data in the literature [42,8]. In this study, the details of the feed composition and properties of the components that are involved (see Table 3) are taken from Long et al. [8]. The feed stream considered in this work is fed at 41.36 bar as saturated liquid, with a temperature of 85 °C. The feed flow is chosen to be 1.7641 kmol/s (which is equivalent to 100,000 BPD). The relative volatility of the feed at these conditions is shown in Table 4. It can be observed that the most difficult separation is between i-butane and n-butane. Several utilities are used for heating, cooling, and refrigeration, as listed in Table 5. The prices of utilities are taken from Turton et al. [45].

There are 5 product streams with various recoveries (given in %, listed in Table 6) taken from Long et al. [8]. It is assumed that demethanization (separation of methane and later components) has already taken place.

- *Product A* – ethane (94.57% recovery), propane (4.96%) and methane (100%)
- *Product B* – propane (94.97%), ethane (5.43%), i-butane (7.44%)
- *Product C* – i-butane (83.62%), propane (0.07%) and n-butane (0.27%)
- *Product D* – n-butane (98.93%), i-pentane (3.11%) and i-butane (8.94%)
- *Product E* – i-pentane (96.89%), n-butane (0.8%), n-pentane (100%), C6&C7 (100%)

Product storage conditions are considered in this study. All products are obtained in the liquid phase with the pressure at 3.5 bar (50 psi) above respective vapor pressure: Ethane at a temperature of −30 °C, 14.16 bar; Propane at 38 °C, 16.55 bar; i-Butane at 38 °C, 8.47 bar; n-Butane at 38 °C, 7.04 bar; Condensate at 38 °C, 4.94 bar (GPSA Standard 2140) [46]. Fig. 7 shows the vapor pressure – temperature profile for pure ethane, propane, isobutane, n-butane and i-pentane products taken

Table 6
Component recoveries (%) in NGL products.

Component Recoveries %	Ethane product	Propane product	i-Butane product	n-Butane Product	Gasoline product	Recovery sum
Methane	100					100
Ethane	94.57	5.43				100
Propane	4.96	94.97	0.07			100
i-Butane		7.44	83.62	8.94		100
n-Butane			0.27	98.93	0.8	100
i-Pentane				3.11	96.89	100
n-Pentane					100	100
n-Hexane					100	100
n-Heptane					100	100

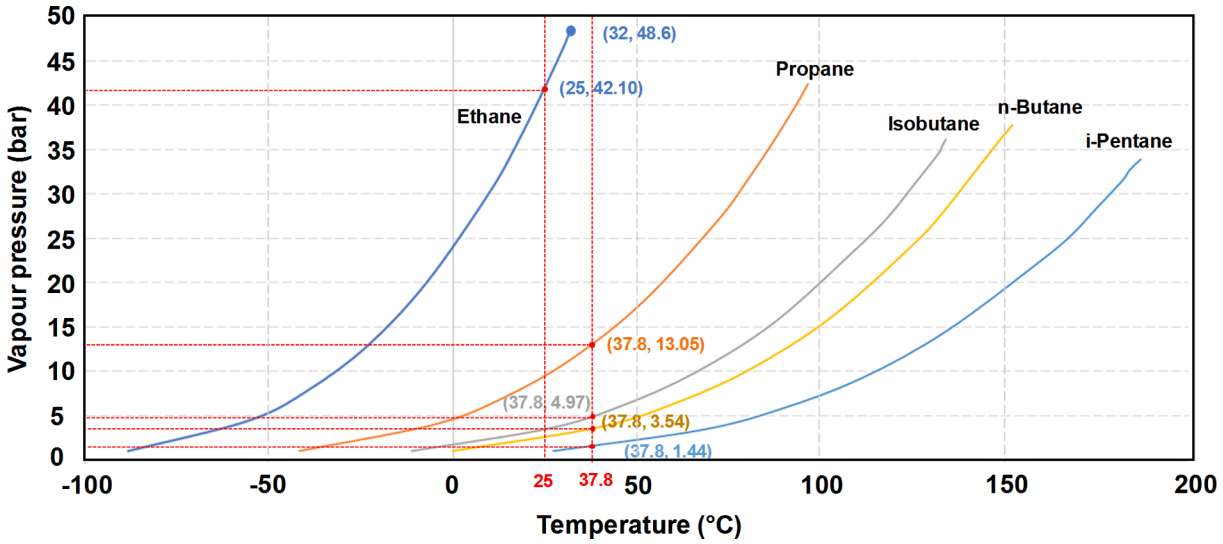

Fig. 7. Vapor pressure – Temperature profile for NGL products.

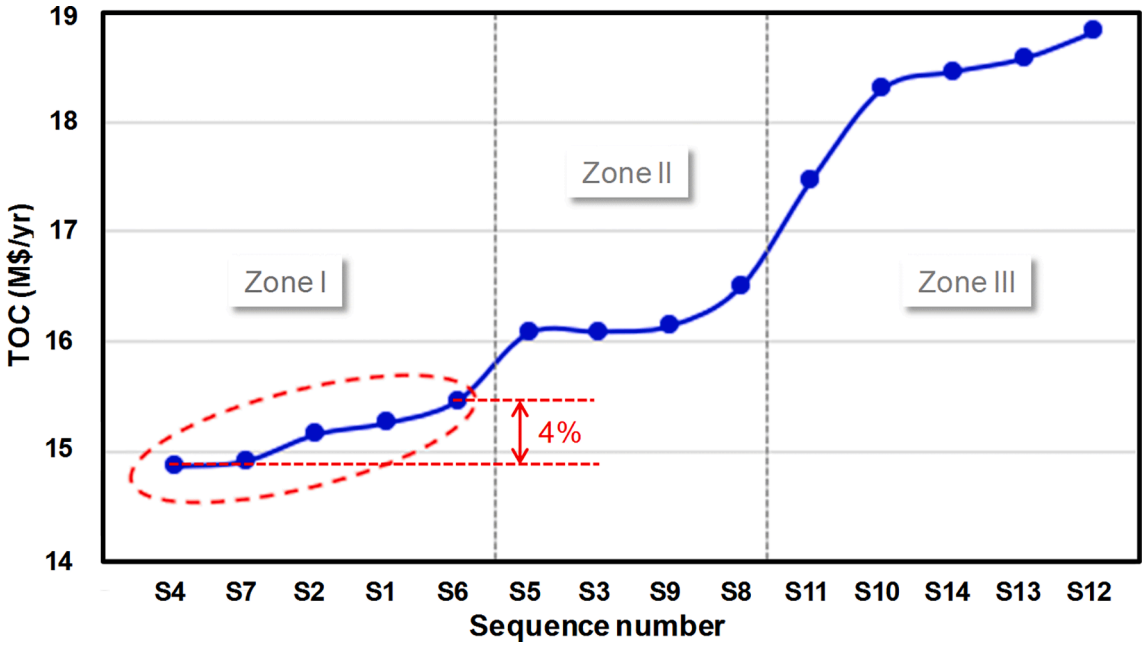

Fig. 8. Total operating costs ranking of simple column sequences.

from Aspen Plus.

For optimization, there are 14 possible sequences of 4 simple columns (counting from S1 = direct to S14 = indirect, as listed in Fig. 1) when fixing the topology of the base sequence in each case. Afterwards, the complex cases are optimized from the same simple starting point and defaults, leading to another set of 14 sequences (C1–C14) generated for a mixture of 5 products. These sequences are generated by three optimization routes: (1) sequences without heat integration; (2) heat

Table 7
Comparison between shortcut models and rigorous simulation results of sequence 7.

	Column 1 (AB/CDE)		Column 2 (A/B)		Column 3 (CD/E)		Column 4 (C/D)	
	SC*	R*	SC	R	SC	R	SC	R
Vapor frac	0.39	0.39	0.98	0.98	0.65	0.65	0.99	0.99
Pressure (bar)	21.28	21.28	17.15	17.15	4.61	4.61	4.62	4.62
T_{feed} (°C)	51.44	51.04	21.49	22.26	68.22	67.94	44.36	44.34
Condenser type	Partial		Total		Partial		Total	
T_{conden}(°C)	30.2	31.0	−17.0	−17.0	44.4	44.4	34.4	34.9
T_{reb}(°C)	133.2	132.9	43.3	43.7	97.7	97.2	47.1	47.1
Condenser duty (MW)	18.78	16.31	20.36	22.63	10.30	10.52	25.29	26.75
Reboiler duty (MW)	30.16	27.73	5.91	8.04	10.03	10.23	18.51	20.14
Reflux ratio	1.22	1.05	1.59	1.88	1.50	1.56	13.15	13.97
Number of stages**	39	39	15	15	27	27	67	67
Feed stage**	9	9	9	9	13	13	51	51

Note: * SC refers to shortcut models, R refers to rigorous model; ** Theoretical stages.

Table 8
Comparison between real relative volatilities* versus the geometric mean α in the shortcut models of sequence 7.

	Column 1 (AB/CDE)		Column 2 (A/B)		Column 3 (CD/E)		Column 4 (C/D)	
	SC	R	SC	R	SC	R	SC	R
Top stage	1.98	2.08	3.65	3.62	2.22	2.13	1.34	1.34
Bottom stage	1.46	1.49	2.46	2.47	1.87	1.89	1.33	1.33
Log mean α**	1.70	n/a	3.00	n/a	2.04	n/a	1.34	n/a

Note: * Real relative volatilities between LK and HK components at the top and bottom stage of the columns generated by rigorous simulations; ** Log mean relative volatility $\alpha = (\text{top } \alpha \times \text{bottom } \alpha)^{-0.5}$.

Table 9
Cost comparison between non-heat integrated simple and complex columns.

Seq. No.	Simple sequences		Complex sequences		TOC Savings %
	TOC (M $/yr)	TIC* (M $/yr)	TOC (M $/yr)	TIC* (M $/yr)	
1	15.26	5.05	12.79	5.49	16%
2	15.15	6.10	12.97	4.13	14%
3	16.09	5.72	14.82	4.40	8%
4	14.86	5.00	12.79	5.49	14%
5	16.07	6.68	14.27	6.33	11%
6	15.46	6.35	12.78	5.53	17%
7	14.91	6.23	12.78	5.50	14%
8	16.50	7.57	14.78	10.65	10%
9	16.14	9.20	12.78	5.56	21%
10	18.30	7.81	15.01	4.54	18%
11	17.47	8.34	16.28	7.62	7%
12	18.82	9.21	15.50	11.26	18%
13	18.58	7.71	14.84	4.51	20%
14	18.46	10.66	15.88	11.02	17%

* **Note**: TIC is the annualized total investment cost, estimated relative to the end of year 2021 (CEPCI index = 776.9), assuming a loan repayment period of 10 years and interest rate of 5%.

Table 10
Optimal column sequences based on simple (S) and complex (C) columns.

Seq.	Vapor rate (kmol/s)	TOC (M $/yr)	Sav^1 (%)	TOC Ranking	Sav^2 (%)	TIC* (M $/yr)
S1	6.51	12.18	20%	10	n/a	14.25
S2	6.61	13.55	11%	16		14.32
S3	6.56	11.89	26%	7		14.72
S4	4.83	11.13	25%	1		5.68
S5	4.21	14.36	11%	22		8.12
S6	5.08	12.14	22%	9		9.56
S7	5.09	12.30	17%	11		6.78
S8	5.06	14.44	12%	23		9.12
S9	6.64	15.01	7%	25		14.07
S10	6.50	14.48	21%	24		11.99
S11	7.43	13.93	20%	18		20.64
S12	5.41	16.75	11%	27		9.46
S13	6.05	15.25	18%	26		12.55
S14	5.37	17.24	7%	28		10.48
C1	3.69	11.54	10%	6	5%	4.36
C2	3.76	11.53	11%	5	15%	4.28
C3	3.69	12.08	18%	8	−2%	5.98
C4	4.84	11.13	13%	1	0%	5.68
C5	4.93	12.40	13%	13	14%	6.98
C6	3.87	11.38	11%	3	6%	5.49
C7	5.10	12.30	4%	11	0%	6.78
C8	5.92	14.16	4%	20	2%	11.62
C9	3.84	11.38	11%	3	24%	5.47
C10	5.38	13.51	10%	14	7%	10.04
C11	7.43	13.93	14%	18	0%	20.64
C12	4.43	14.25	8%	21	15%	11.45
C13	5.38	13.51	9%	14	11%	10.04
C14	4.38	13.78	10%	17	20%	7.30

Note: Sav^1 (%) represents the savings of the heat integrated sequences compared to the non-heat integrated sequences, while Sav^2 (%) represents the savings of heat-integrated complex sequences compared to the heat-integrated simple sequences. TIC is the annualized total investment cost, estimated relative to the end of year 2021 (CEPCI index = 776.9), assuming a loan repayment period of 10 years and interest rate of 5%.

integrated sequences based on Pinch Analysis; and (3) heat integrated sequences with heat exchanger network design. The optimization is carried out using a desktop PC with *CPU - Intel(R) Core i7-10700 CPU 2.90 GHz* (8 cores), with an average time resource of 19 h.

5. Results and discussion

5.1. Optimization results evaluation and analysis

A series of optimizations was carried out to explore the optimal arrangement for the NGL separation. Firstly, the non-energy integrated sequences are carried out by optimizing the operating design variables using simple columns. Fig. 8 provides the total operating cost rankings of the 14 sequences in descending order. Taking into account the actual operating conditions and the operational flexibility, the best few sequences should be kept for further detailed design rather than the best single sequence [30]. In this case, the first sequence family, which are the 5 top ranked sequences (Zone-I), are considered the most economically attractive sequence family identified by the screening method based on shortcut models. To evaluate the performance of these proposed sequences and the ability to find reliable economically attractive sequences with the shortcut-based screening method, the simple column sequences are validated by rigorous simulations carried out using the Aspen Plus RadFrac model, with the short-cut design details (reflux ratio, trays, condenser temperatures and distillate rate) extracted as the initialization parameters for the rigorous simulations. Defining the best

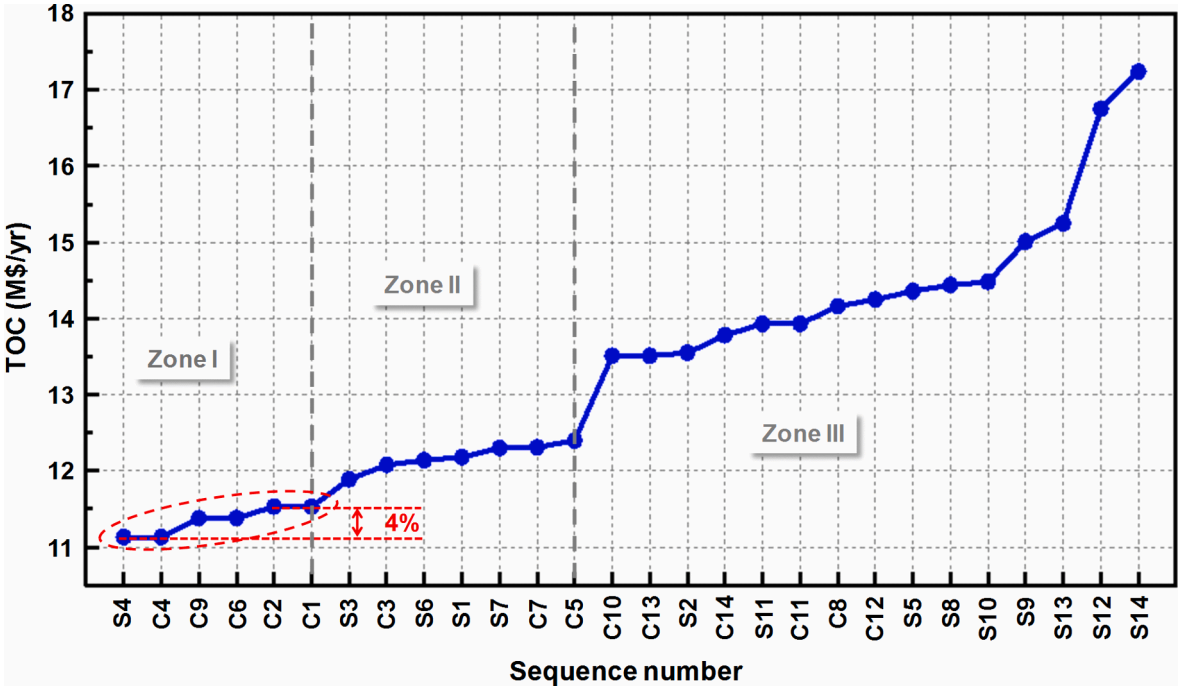

Fig. 9. Sequence rankings of simple and complex columns in terms of total operating cost.

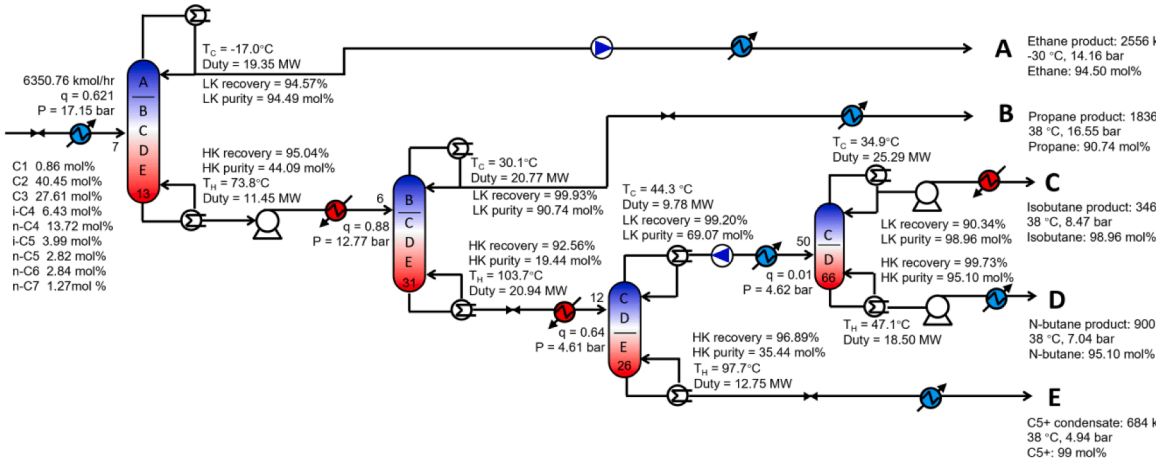

Fig. 10. Optimised operating conditions of the non-heat integrated simple sequence 4.

few sequences within a 10% difference in the total operating costs as the most economically attractive sequences subset [12], S7 is the most economically attractive sequence identified by rigorous simulations, followed by S6 and then S4. It should be noted that in the economically attractive S6, the most difficult pair to separate, C/D, is not separated as a binary pair, but is separated as C/DE. This is because the presence of other components increases the relative volatility between the key components, making the separation between the close boiling binary pair easier, and reducing the energy required. When getting benefits from the presence of other non-key components, the column pressure should not be very high as increasing column pressure decreases the relative volatilities. The column pressure of the C/DE column is 4.62 bar.

Table 7 provides details of the rigorous simulation results and a comparison with the shortcut methods of sequence 7 as an example. Additional information on the real relative volatility (α) values at the top and bottom stage of the columns by rigorous simulations versus the geometric mean α in shortcut models of sequence 7 is provided in Table 8, which shows the actual variation of the α across stages. The relevant details of sequence 6 and sequence 4 can be found in Appendix B. The three most promising sequences identified by rigorous simulations have all been preselected within the attractive families by the pre-screening based on the developed approach, indicating that despite the deviation between shortcut and rigorous models, the developed fast screening method using shortcut models is validated. The following comparisons are given based on the developed screening results.

5.2. *Energy integrated distillation sequences*

Energy intensified sequences using complex columns and heat integration bring significant energy benefits. Table 9 provides the TOC comparison between non-heat integrated simple and complex columns. It shows that all the non-heat integrated simple sequences benefit, in terms of total operating cost savings, from introducing complex columns within the range of 7–21%. The sequence with the lowest TOC is now the complex sequence 6, which separates isobutane by a side rectifier, followed by two simple columns separating ethane/propane and n-butane/

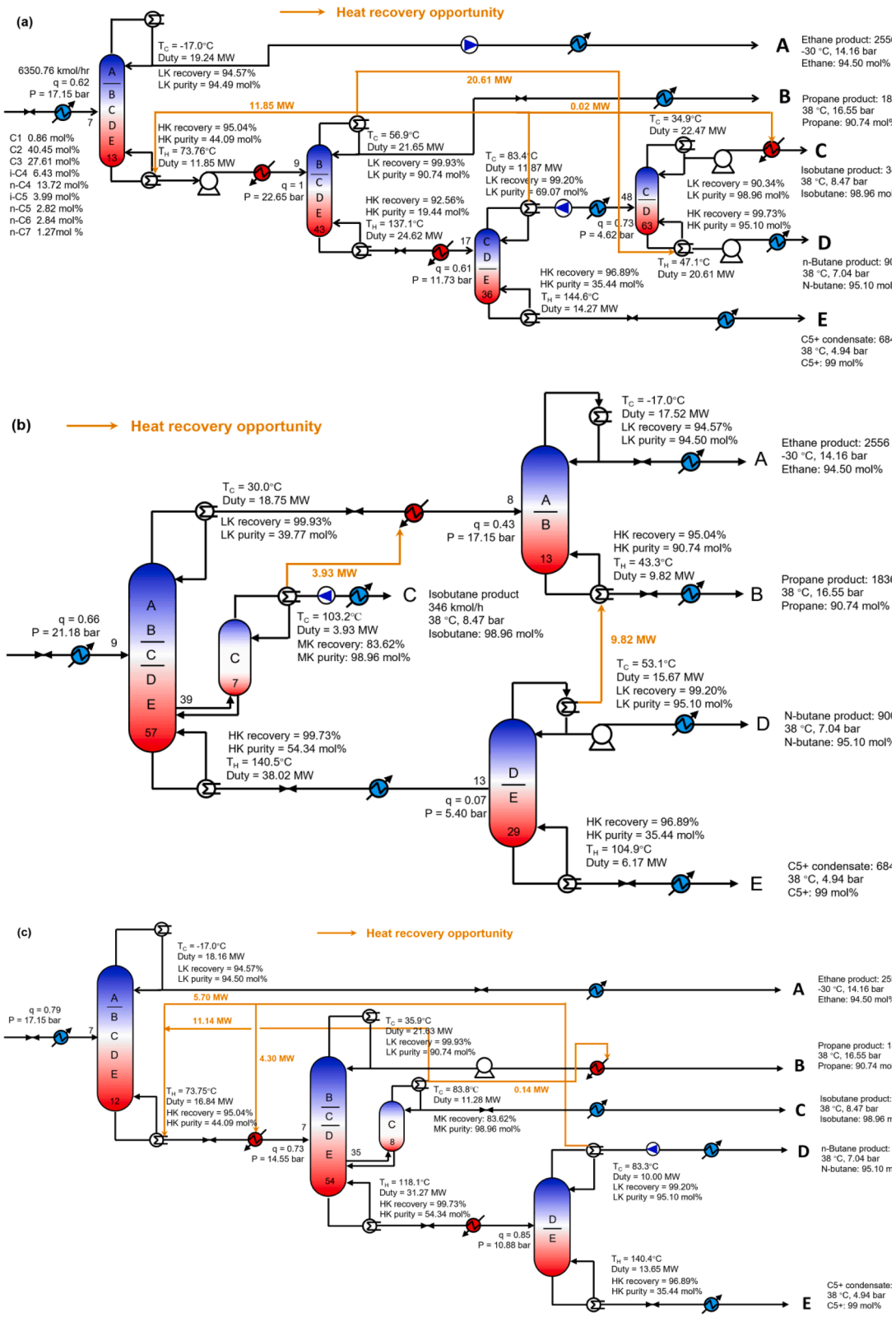

Fig. 11. Details of the Top 3 attractive distillation sequence designs (a) S4, (b) C9, (c) C2.

C5+, with the TOC of 12.78 M$/yr. Compared with its corresponding simple sequence S6, the requirement of the refrigerant remains the same, but the reboiler duty (LP steam requirement) decreased from 68 MW to 51 MW, and the condenser duty (required of cooling water) decreased from 59 MW to 37 MW.

To achieve further energy savings, heat integration is applied, achieved by optimizing the heat exchanger network with column operating conditions simultaneously for both simple and complex sequences. Table 10 lists the optimal heat integrated column sequences based on simple (S) and complex (C) columns. The total operating cost saving brought by heat integration on the optimized non-heat integrated simple columns is up to 26%, and the operating cost saving from

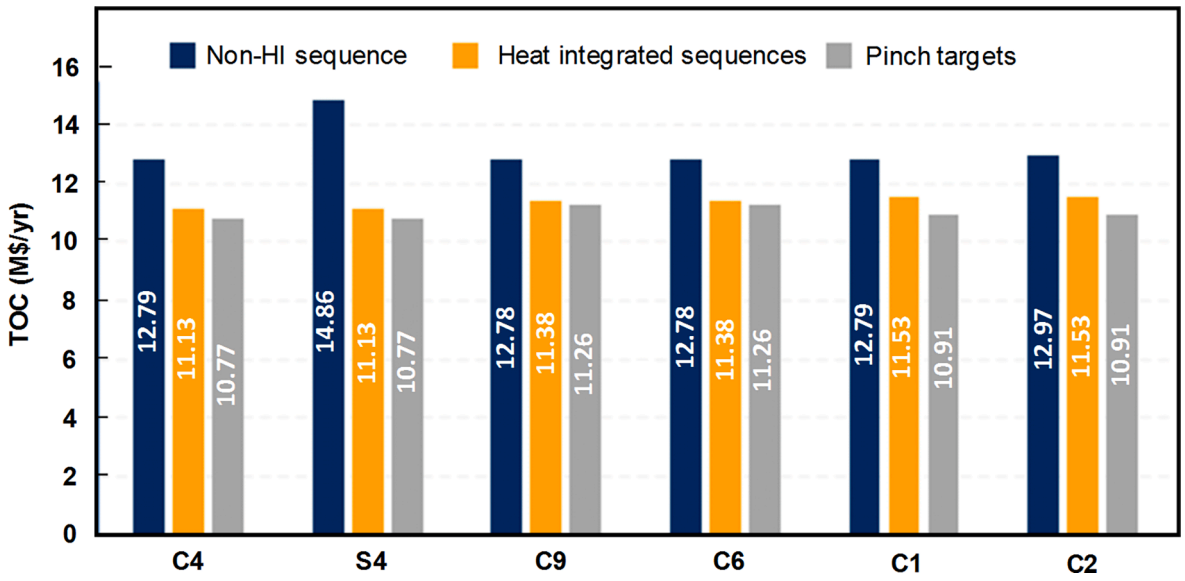

Fig. 12. Comparison of total operating costs among different design scenarios.

Table B1
Comparison between shortcut models and rigorous simulation results of S6.

	Column 1 (AB/CDE)		Column 2 (A/B)		Column 3 (C/DE)		Column 4 (D/E)	
	SC*	R*	SC	R	SC	R	SC	R
Vapor frac	0.39	0.39	0.98	0.98	0.64	0.64	0.10	0.10
Pressure (bar)	21.20	21.20	17.15	17.15	4.62	4.62	3.27	3.27
T_{feed} (°C)	51.3	50.9	21.5	22.3	68.1	67.8	50.6	50.2
Condenser type	Partial		Total		Total		Total	
T_{conden}(°C)	30.0	30.8	−17.0	−17.0	34.9	35.0	34.6	34.6
T_{reb}(°C)	133.0	132.7	43.3	43.7	62.9	62.5	83.1	82.5
Condenser duty (MW)	18.76	16.28	20.37	22.63	27.25	29.91	12.97	12.32
Reboiler duty (MW)	30.12	27.69	5.91	8.04	19.50	22.25	12.68	12.02
Reflux ratio	1.22	1.04	1.59	1.88	14.24	15.74	1.50	1.42
Number of stages**	39	39	15	15	68	68	24	24
Feed stage**	9	9	9	9	50	50	12	12

Note: * SC refers to shortcut models, R refers to rigorous model; ** Theoretical stages.

Table B2
Comparison between real relative volatilities* versus the geometric mean α in shortcut models of S6.

	Column 1 (AB/CDE)		Column 2 (A/B)		Column 3 (C/DE)		Column 4 (D/E)	
	SC	R	SC	R	SC	R	SC	R
Top stage	1.99	2.09	3.65	3.62	1.34	1.34	2.34	2.23
Bottom stage	1.46	1.49	2.46	2.47	1.30	1.28	1.98	2.00
Log mean α**	1.71	n/a	3.00	n/a	1.32	n/a	2.15	n/a

Note: * Real relative volatilities between LK and HK components at the top and bottom stage of the columns generated by rigorous simulations; ** Log mean α = (top α × bottom α)$^{-0.5}$.

optimizing both heat integration and complex columns can achieve up to 38%. It should be noted that the heat integration between heat sources and heat sinks used for the sequences in this table is constrained such that each source of heat was matched with a maximum of two heat sinks and each heat sink was matched with a maximum of two heat sources. This constraint avoids the heat exchanger network becoming overly complex. Removing the constraint will decrease the utility cost at the expense of increased capital cost. However, the increase in capital cost will not be reflected accurately in approximate capital cost estimation methods used for calculation. Restricting the heat sources and sinks to a maximum of two matches is considered to be a practical constraint for the vast majority of cases.

Fig. 9 shows the overall ranking of heat integrated simple and complex column sequences in terms of total operating costs. Simple sequence 4 is ranked the best (with the detailed design in Fig. 10) when optimizing heat integration and complex column arrangements, with the total operating cost of 11.13 M$/yr, and a 25% total operating cost saving is achieved compared to the optimum non-heat integrated simple sequence, as shown in Figs. 11 and 12. Based on the results, simple column sequences benefit to a larger extent from heat integration compared to complex column sequences, which can achieve an average energy saving of 16% by introducing heat integration, but complex columns gain an average 11% energy saving compared to the optimum non-heat integrated complex columns sequences in this case study. This is because complex columns reduce the number of design degrees of freedom compared with the non-combined two adjacent simple columns, for example, the column pressures do not need to be the same for two simple columns if they are not to be merged into one complex column. Complex columns therefore lose some potential heat integration possibilities after merging simple columns as the combination of heat sinks and sources are constrained. The potential benefits of lower capital costs that could be obtained from using complex columns are not taken into account in the optimization (which focused on minimizing TOC), as the capital costs may not be reflected accurately using cost correlations methods. Nonetheless, the potential advantages in terms of capital cost can be also evaluated based on the additional TIC data provided in

Table B3
Comparison between shortcut models and rigorous simulation results of S4.

	Column 1 (A/BCDE)		Column 2(B/CDE)		Column 3(CD/E)		Column 4 (C/D)	
	SC*	R*	SC	R	SC	R	SC	R
Vapor frac	0.45	0.45	0.13	0.13	0.40	0.40	0.99	0.99
Pressure (bar)	17.15	17.15	12.77	12.77	4.61	4.61	4.62	4.62
T_{feed} (°C)	44.0	43.6	62.1	61.6	62.3	62.0	44.4	44.4
Condenser type	Total	Total	Partial	Total				
T_{conden}(°C)	−17.0	−16.9	30.1	30.6	44.3	44.3	34.9	34.9
T_{reb}(°C)	73.8	73.3	103.7	103.5	97.7	97.2	47.1	47.1
Condenser duty (MW)	19.35	23.79	20.77	21.78	9.78	9.50	25.29	26.66
Reboiler duty (MW)	11.45	15.86	20.94	21.92	12.75	12.40	18.50	20.08
Reflux ratio	1.46	2.03	1.85	1.93	1.43	1.41	13.15	13.93
Number of stages**	14	14	32	32	26	26	66	66
Feed stage**	8	8	7	7	12	12	50	50

Note: * SC refers to shortcut models, R refers to rigorous model; ** Theoretical stages.

Table B4
Comparison between real relative volatilities* versus the geometric mean α in shortcut models of S4.

	Column 1 (A/BCDE)		Column 2 (B/CDE)		Column 3 (CD/E)		Column 4 (C/D)	
	SC	R	SC	R	SC	R	SC	R
Top stage	3.65	3.62	2.14	2.27	2.22	2.13	1.34	1.34
Bottom stage	2.21	2.20	1.69	1.73	1.87	1.89	1.33	1.33
Log mean α**	2.84	n/a	1.90	n/a	2.04	n/a	1.34	n/a

Note: * Real relative volatilities between LK and HK components at the top and bottom stage of the columns generated by rigorous simulations; ** Log mean α = (top α × bottom α)$^{-0.5}$.

Table 10 for each of the optimal sequences.

The top 6 sequences with rather small operating cost differences (within 5%) are considered the most economically attractive sequence family (and it remains so, even when TIC is also factored in). It should be noted that when introducing heat integration, applying complex columns cannot provide benefits for sequence 4, and thus the optimum design for S4 and C4 are the same. The final designs of heat integrated C6 and C9 are the same, C1 and C2 are the same, by merging different columns in S6 and S9; S1 and S2. Overall, the recommended economic attractive sequences for the NGLs fractionation process in terms of total operating cost are, in order: S4 (C4), C6 (C9), and C1 (C2). The optimum configurations with design details of these three sequences are shown in Fig. 11. Depending on the parameters used for optimization, there might be slight changes in the ranking of these sequences. It is worth noting that the complex distillation sequences proposed involve indeed highly integrated thermally coupled columns or dividing-wall columns, but these can be effectively well controlled provided that an appropriate control structure is used [47].

In order to compare the difference between the heat integration achieved by actual heat exchanger network design and the Pinch Analysis targets, the heat integration of simple and complex sequences is also carried out. Fig. 12 presents the operating cost details for the three most attractive heat-integrated sequences, and their non-heat integrated sequences, as well as the difference between heat exchanger network design with practical constraints and the heat integration targets achieved by Pinch Analysis. It should be noted that the column pressure will increase if process to process heat integration is introduced. For example, according to the operating details given in Fig. 11, the pressures of column 2 (B/CDE) and 3 (CD/E) are increased from 12.77 bar to 22.65 bar and from 4.61 bar to 11.73 bar respectively, compared to the non-heat integrated column in order to achieve hot enough condenser temperatures to transfer heat to other heat sinks.

Overall, the design of S4 (Fig. 11) is the best sequence and consists of a simple column that splits A/BCDE, followed by a simple column that separates B/CDE, and then two columns that separate CD/E and C/D, respectively, with heat integration opportunities. The design of C6 (Fig. 11) is the next best and consists of a side-rectifier separating AB/C/DE, followed by two simple columns that splits A/B and D/E. Then is the design of C1 that consists of a simple column splitting A/BCDE, followed by a side-rectifier separating B/C/DE, and then another simple column separates D/E.

5.3. Sustainability metrics

The sustainability of the process can be evaluated using several metrics: material and energy intensity, water consumption, toxic and pollutant emissions, greenhouse gas (GHG) emissions – with lower values meaning better performance [48]. The following evaluations are carried out based on the best heat integrated distillation sequence S4 (C4).

- *Material intensity* expresses the mass of wasted materials per unit of output. In this separation process, there are five outlet streams, and all five are product streams. Therefore, there is zero kg waste in this process.
- *Energy intensity* represents the primary energy consumed per unit of output (i.e. per kg of all NGL products). The heat integrated process S4 and C4 requires total heating of 41,786 kW / 284,679 kg/h = 0.15 kWh/kg NGL products (0.53 MJ/kg NGL products) and total cooling of −55,330 kW / 284,679 kg/h = -0.19 kWh/kg NGL products (0.70 MJ/kg NGL products).
- *Water consumption* expresses the amount of water used per unit of output. The temperature range from process to cooling tower is 5 °C, from 20 to 25 °C. The cooling capacity of water is 4.187 kJ/kgK . The flowrate of CW is 6052 m^3/h. As water cooling is obtained by evaporation in cooling towers, the loss must be compensated by a make-up with fresh water. Following the 7% rule [48], the total water loss is 0.07 × 6052 = 423.6 m^3/h (or 0.0015 m^3/kg NGL).
- *Greenhouse gas (GHG) emissions* expresses the total GHG emitted per unit of output. This amount is proportional to the energy used in the process. Based on the US-EPA-RULE-E9-5711 method, the CO_2 emission factor given by Aspen Plus for natural gas is 5.589 × 10^{-8} kg CO_2 / J, and the default CO_2 energy source efficiency factor is 1. Considering the energy intensity (0.53 MJ/kg NGL products), the specific CO_2 emissions are 0.030 kg CO_2 / kg NGL products, translated to 8,432.68 kg/h CO_2.

6. Conclusions

The systematic screening approach developed in this study was successfully used for simultaneously optimizing sequence structures, accounting for all design degrees of freedom and heat integration in the distillation sequences. By optimizing the whole sequencing process, novel NGL fractionation sequences have been explored and ranked

techno-economically. The generated economically attractive sequences (ranked by the operating costs) are shown to be comparable with those of rigorous simulations using the Aspen Plus RadFrac model. For a given feed composition and product requirements, the ranking of the designed energy integrated complex sequences for the NGL fractionation are listed, and the most energy efficient economically attractive sequence family has been selected. The best sequences in terms of total operating costs are presented, with total operating costs of 11.13, 11.38 and 11.53 M$/yr, respectively, for a processed NGL feed rate of 6350.76 kmol/hr (2,500 kton per year). These results demonstrate that screening of the search space of energy-efficient distillation sequences considering synthesis and optimization of all the design degrees of freedom is achievable with the newly proposed approach.

7. Author statement

All persons who meet authorship criteria are listed as authors, and all authors certify that they have participated sufficiently in the work to take public responsibility for the content, including participation in the concept, design, analysis, writing, or revision of the manuscript. Furthermore, each author certifies that this material or similar material has not been and will not be submitted to or published in any other publication.

CRediT authorship contribution statement

Qing Li: Conceptualization, Methodology, Software, Data curation, Validation, Visualization, Writing – original draft, Writing – review & editing. **Adrian J. Finn:** Conceptualization, Methodology, Validation, Writing – review & editing. **Stephen J. Doyle:** Methodology, Formal analysis, Investigation, Validation. **Robin Smith:** Conceptualization, Methodology, Formal analysis, Investigation, Validation, Supervision, Writing – review & editing. **Anton A. Kiss:** Conceptualization, Methodology, Formal analysis, Investigation, Resources, Visualization, Validation, Supervision, Project administration, Writing – original draft, Writing – review & editing.

Declaration of Competing Interest

The authors declare that they have no known competing financial interests or personal relationships that could have appeared to influence the work reported in this paper.

Data availability

Data will be made available on request.

Acknowledgements

All persons who have made substantial contributions to the work reported in the manuscript (e.g., technical help, writing and editing assistance, general support), but who do not meet the criteria for authorship, are named in the Acknowledgements and have given us their written permission to be named. If we have not included an Acknowledgements, then that indicates that we have not received substantial contributions from non-authors.

Appendix A. . Flow charts on the models of multistage-compressors and turbo expanders

A.1 Multi-stage isentropic compressor

A.1.1 Inputs

(1) P_in / bar – inlet pressure
(2) P_out / bar – outlet pressure
(3) T_in / K – inlet temperature
(4) Molar Composition (in molar fraction)
(5) CMPR_EFF – stage isentropic efficiency
(6) Pr.max – maximum stage pressure ratio

A.1.2 Number of stages - N_stage

N_stage = log(Pout/Pin)/log(Pr.max)
Pr.max > (Pout/Pin)^(1/N_stage)

A.1.3 The flowchart of the method

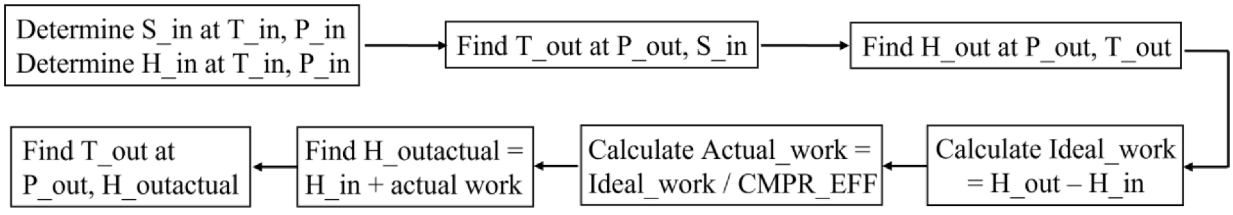

If T_out for the stage > T_ambient utility + DTmin, then the vapor stream is cooled to T_ambient utility + DTmin.
P_in_stage (n + 1) = P_out_stage (n)
T_in_stage(n + 1) = T_out.stage(n)
Any liquid form is separated and compressed using an isentropic liquid pump, and the vapor flowrate of the remaining stages is subsequently reduced. The liquid is combined with the final outlet vapor to give the over composition and temperature.

A.2 Turbo expander – Generates power from pressure reduction

A.2.1 Inputs

(1) P_in / bar – inlet pressure
(2) P_out / bar – outlet pressure
(3) T_in / K – inlet temperature
(4) Molar Composition (in molar fraction)
(5) ISEN_EFF – stage isentropic efficiency

A.2.2 The flowchart of the method

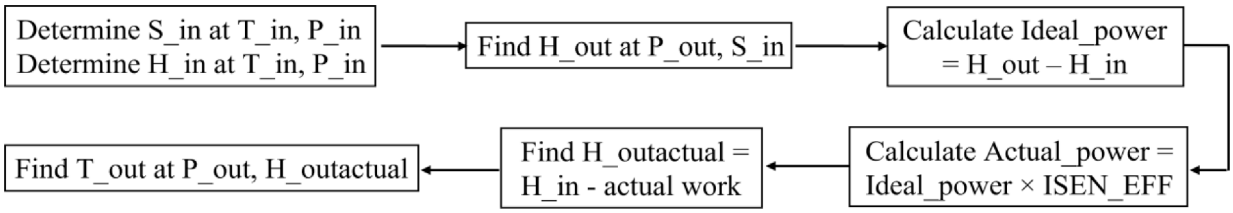

Appendix B. . Operating condition details of sequence 6 and sequence 4

See Tables B1, B2, B3 and B4.

References

[1] J.D. Seader, A.W. Westerberg, A combined heuristic and evolutionary strategy for synthesis of simple separation sequences, AIChE J 23 (1977) 951–954.
[2] M.J. Andrecovich, A.W. Westerberg, An MILP formulation for heat-integrated distillation sequence synthesis, AIChE J 31 (1985) 1461–1474.
[3] M.O. Bertran, R. Frauzem, A.S. Sanchez-Arcilla, L. Zhang, J.M. Woodley, R. Gani, A generic methodology for processing route synthesis and design based on superstructure optimization, Comput. Chem. Eng. 106 (2017) 892–910.
[4] L. Kong, C.T. Maravelias, New multicomponent distillation costillation network synthesis using superstructure-based methods, Comput. Chem. Eng. 133 (2020), 106650.
[5] A.A. Shenvi, V.H. Shah, R. Agrawal, New multicomponent distillation configurations with simultaneous heat and mass integration, AIChE J 59 (2013) 272–282.
[6] H.Y. Lee, M.H. Yeh, Y.Y. Chen, C.L. Chen, Design and control of a comprehensive ethylenediamine (EDA) process with external/internal heat integration, Sep. Purif. Technol. 293 (2022), 121137.
[7] M. Yang, T. Li, X. Feng, B.G. Rong, Y. Wang, Retrofit of an industrial solvent recovery system: Distillation sequence intensification and simulation-based optimization, Chem. Eng. Res. Des. 180 (2022) 164–177.
[8] N.V.D. Long, L.Q. Minh, T.N. Pham, A. Bahadori, M. Lee, Novel retrofit designs using a modified coordinate descent methodology for improving energy efficiency of natural gas liquid fractionation process, J. Nat. Gas Sci. Eng. 33 (2016) 458–468.
[9] R. Premkumar, G.P. Rangaiah, Retrofitting conventional column systems to dividing-wall columns, Chem. Eng. Res. Des. 87 (2009) 47–60.
[10] D. Zhang, S. Zeng, Z. Li, M. Yang, X. Feng, Simulation-assisted design of a distillation train with simultaneous column and sequence optimization, Comput. Chem. Eng. 164 (2022), 107907.
[11] D. Leeson, P. Fennell, D.N. Mac, N. Shah, Simultaneous design of separation sequences and whole process energy integration, Chem. Eng. Res. Des. 125 (2017) 166–180.
[12] G.M. Ramapriya, A. Selvarajah, L.E. Jimenez Cucaita, J. Huff, M. Tawarmalani, R. Agrawal, Short-cut methods versus rigorous methods for performance-evaluation of distillation configurations, Ind. Eng. Chem. Res. 57 (2018) 7726–7731.
[13] H. Yoo, M. Binns, M.G. Jang, H. Cho, J.K. Kim, A design procedure for heat-integrated distillation column sequencing of natural gas liquid fractionation processes, Korean J. Chem. Eng. 33 (2016) 405–415.
[14] R. Smith, C. Triantafyllou, The design and optimisation of fully thermally coupled distillation columns, Trans. IChemE 70 (1992) 118–132.
[15] O.A. Flores, J.C. Cárdenas, S. Hernández, V. Rico-Ramírez, Thermodynamic analysis of thermally coupled distillation sequences, Ind. Eng. Chem. Res. 42 (2003) 5940–5945.
[16] I.J. Halvorsen, I. Dejanović, K.A. Maråk, Ž. Olujić, S. Skogestad, Dividing-wall column for fractionation of natural gas liquids in floating liquefied natural gas plants, Chem. Eng. Technol. 39 (2016) 2348–2354.
[17] N.V.D. Long, M. Lee, Improvement of natural gas liquid recovery energy efficiency through thermally coupled distillation arrangements, Asia Pac. J. Chem. Eng. 7 (2012) S71–S77.
[18] F. Lestak, C.J.C.E. Collins, Advanced distillation saves energy and capital 104 (1997).
[19] R. Agrawal, Z.T. Fidkowski, Are thermally coupled distillation columns always thermodynamically more efficient for ternary distillations? Ind. Eng. Chem. Res. 37 (1998) 3444–3454.
[20] T. Waltermann, M. Skiborowski, Efficient optimization-based design of energy-integrated distillation processes, Comput. Chem. Eng. 129 (2019), 106520.
[21] M.J.C.E. Skiborowski, Fast screening of energy and cost efficient intensified distillation processes 69 (2018).
[22] R.N.S. Rathore, K.A. Van Wormer, G.J. Powers, Synthesis strategies for multicomponent separation systems with energy integration, AIChE J 20 (1974) 491–502.
[23] W. An, X. Yuan, A simulated annealing-based approach to the optimal synthesis of heat-integrated distillation sequences, Comput. Chem. Eng. 33 (2009) 199–212.
[24] S. Zhang, Y. Luo, X. Yuan, Synthesis of simultaneously heat integrated and thermally coupled nonsharp distillation sequences based on stochastic optimization, Comput. Chem. Eng. 127 (2019) 158–174.
[25] S. Zhang, Y. Luo, X. Yuan, A novel stochastic optimization method to efficiently synthesize large-scale nonsharp distillation systems, AIChE J 67 (2021) e17328.
[26] A.A. Kiss, R. Smith, Rethinking energy use in distillation processes for a more sustainable chemical industry, Energy 203 (2020), 117788.
[27] R.T. Gooty, R. Agrawal, M. Tawarmalani, Advances in MINLP to identify energy-efficient distillation configurations, Oper. Res. (2022). doi: 10.1287/opre.2022.2340.
[28] Z. Jiang, R. Agrawal, Process intensification in multicomponent distillation: a review of recent advancements, Chem. Eng. Res. Des. 147 (2019) 122–145.
[29] W.D. Seider, J.D. Seader, D.R. Lewin, Process Design Principles: Synthesis, Analysis, and Evaluation, John Wiley & Sons, New York, 1999.
[30] Smith R., Chemical process design and integration, Second edition. ed., John Wiley & Sons, Inc., Chichester, West Sussex, United Kingdom, 2016.
[31] M.R. Fenske, Fractionation of Straight-Run Pennsylvania Gasoline, Ind. Eng. Chem. 24 (1932) 482–485.
[32] E.R. Gilliland, Multicomponent rectification estimation of the number of theoretical plates as a function of the reflux ratio, Ind. Eng. Chem. 32 (1940) 1101–1106.
[33] A.J.V. Underwood, Fractional Distillation of Multicomponent Mixtures, Ind. Eng. Chem. 41 (1949) 2844–2847.
[34] J. Cerda, A.W. Westerberg, D. Mason, B. Linnhoff, Minimum utility usage in heat exchanger network synthesis A transportation problem, Chem. Eng. Sci. 38 (1983) 373–387.
[35] S. Jain, R. Smith, Synthesis of heat-integrated distillation sequence systems, J. Taiwan Inst. Chem. Eng. 43 (2012) 525–534.
[36] A.A. Kiss, C.A. Infante Ferreira, Heat Pumps in Chemical Process Industry, Taylor & Francis, US, 2016.
[37] S. Farrokpanah, Design of heat integrated low temperature distillation systems. The University of Manchester, 2009.
[38] A.M. Gerrard, Guide to Capital Cost Estimating, fourth ed., IChemE, UK, 2000.
[39] CPI Suite, The University of Manchester, Centre for Process Integration, 2022. <www.ceas.manchester.ac.uk/cpi/research/resources/software/> (Date accessed 20 December 2022).

[40] M.B. Franke, Mixed-integer optimization of distillation sequences with Aspen Plus: a practical approach, Comput. Chem. Eng. 131 (2019), 106583.
[41] International Energy Agency - Projections for Natural Gas (2018). IEA, 2018.
[42] D.B. Manley, Thermodynamically efficient distillation: NGL fractionation 28 (1998) 211–216.
[43] A. Tamuzi, N. Kasiri, A. Khalili-Garakani, Design and optimization of distillation column sequencing for NGL fractionation processes, J. Nat. Gas Sci. Eng. 76 (2020), 103180.
[44] M.A. Qyyum, A. Naquash, J. Haider, S.A. Al-Sobhi, M. Lee, State-of-the-art assessment of natural gas liquids recovery processes: Techno-economic evaluation, policy implications, open issues, and the way forward, Energy 238 (2022), 121684.
[45] R. Turton, R.C. Bailie, W.B. Whiting, J.A. Shaeiwitz, Analysis, Synthesis and Design of Chemical Processes, Pearson Education, 2018.
[46] GPSA Engineering Data Book, 14th Edition, Gas Processors and Suppliers Association, Tulsa, Oklahoma, USA (2017).
[47] A.A. Kiss, C.S. Bildea, A control perspective on process intensification in dividing-wall columns, Chem. Eng. Process. 50 (2011) 281–292.
[48] J.M. Schwarz, B.R. Beloff, E. Beaver, Use sustainability metrics to guide decision-making, Chem. Eng. Prog. 98 (2002) 58–63.